Volatile Release from Aqueous Solutions under Dynamic Headspace Dilution Conditions

Michèle Marin,[†] Inger Baek,[‡] and Andrew J. Taylor*[,‡]

Division of Food Sciences, University of Nottingham, Sutton Bonington Campus, Loughborough LE12 5RD, United Kingdom, and Institut National Agronomique Paris-Grignon, Laboratoire de Génie et Microbiologie des Procédés Alimentaires (INRA), 78850 Thiverval-Grignon, France

Static equilibrium was established between the gas phase (headspace) and an unstirred aqueous phase in a sealed vessel. The headspace was then diluted with air to mimic the situation when a container of food is opened and the volatiles are diluted by the surrounding air. Because this first volatile signal can influence overall flavor perception, the parameters controlling volatile release under these conditions are of interest. A mechanistic model was developed and validated experimentally. Release of compounds depended on the air−water partition coefficient (K_{aw}) and the mass transport in both phases. For compounds with K_{aw} values $<10^{-3}$, K_{aw} was the factor determining release rate. When K_{aw} was $>10^{-3}$, mass transport in the gas phase became significant and the Reynolds number played a role. Because release from packaged foods occurs at low Reynolds numbers, whereas most experiments are conducted at medium to high Reynolds numbers, the experimentally defined profile may not reflect the real situation.

Keywords: *Volatile; partition coefficient; mass transfer; modeling; Reynolds number*

INTRODUCTION

For aroma compounds to be perceived by consumers, they must be released from the food matrix so they can enter the airways of the nose and come into contact with the olfactory receptors. Consumers can receive several different volatile signals from a food. Prior to consumption, the volatiles are sampled orthonasally, and this first "sniff" often has a major influence on the consumer's overall perception of the product. Volatiles are also released during eating and travel to the olfactory receptors by the retronasal route. In both situations, a combination of physicochemical parameters (such as the partition coefficient and the mass transfer coefficients), along with dynamic factors (such as mixing of the phases and air flow), determines the relative distribution of the volatile compounds between the food and the air phases. Because the relationship can be described in mathematical terms, various models have been proposed to predict the volatile signal that is delivered to the olfactory receptors.

The simplest model is an air−water system at equilibrium, for which K_{aw} and temperature are the determining factors for volatile release. Air−water equilibrium is well-documented [see Taylor (1998) for a review], and the parameter can be determined experimentally [see, for example, Chaintreau et al. (1995)] as well as by calculation using theoretical data (Gemhling et al., 1991). The more complex models, which have been proposed for volatile release during eating, depend on the type of food and the mechanisms by which volatiles are released (e.g., solubilization, melting, emulsion inversion). There are several published accounts (Darling et al., 1986; Overbosch et al., 1991; Plug and Haring, 1994; Harrison, 1998), but, generally, the models have not been validated with experimental data as it has been difficult to monitor volatile release in vivo until recent advances in analytical techniques (Taylor et al., 1999).

The equilibrium conditions used by many workers to calculate K_{aw} are rarely found in real flavor release situations. This paper takes equilibrium a step further by considering how the headspace volatile profile changes as the equilibrium concentrations are disturbed when the headspace is diluted with air. This system relates to the situation in real food products, such as beverages, when a sealed container (volatiles under equilibrium) is opened and the volatiles are diluted by the surrounding air over a period of time. The volatile concentration in the headspace will vary with time and be different for each volatile, as the headspace concentration of each component will depend on the rate at which that component is removed from the air phase and replenished from the aqueous phase. Thus, the actual volatile concentration experienced by a consumer on opening such a container is not a simple linear dilution of the equilibrium concentration, and the volatile profile will also change with time. This paper adopts a modeling approach, followed by experimental validation, to determine the key parameters controlling volatile release.

A simple system containing an aqueous, nonstirred liquid phase was chosen to investigate the release characteristics. Darling et al. (1986) described a similar system to study volatile release from static (i.e., nonstirred) aqueous systems under simulated in-mouth conditions. They concluded that regeneration of the surface layer was the significant factor and that diffusion was insignificant. Their model did not include a partition coefficient term, but the conditions for release were rather specialized and did not relate to the real life system, which we are attempting to model. The mechanistic model we have developed considers each

[†] Institut National Agronomique Paris-Grignon.
[‡] University of Nottingham.

10.1021/jf990470g CCC: $18.00 © 1999 American Chemical Society
Published on Web 10/14/1999

Table 1. Thermodynamic and Analytical Properties of Volatiles at 25 °C

molecule	MW (Da)	cone voltage (V)	vapor pressure $P_i^0(T)$ (Pa)	activity coeff γ_l^∞	Henry's constant $P_i^0(T)\gamma_l^\infty$
acetaldehyde	44.05	20	120000[a]	3.85[d]	4.62E+05
dimethyl sulfide	62.13	20	62980[b]	208[e]	1.31E+07
diacetyl	86.09	24	8283[a]	11[d]	9.11E+04
2,5-dimethylpyrazine	108.14	23	448[c]	22.6[c]	1.01E+04
menthone	154.25	15	44.5[b]	24870[f]	1.11E+06

[a] Gemhling et al. (1991). [b] Lee-Kesler-Joback method (Reid et al., 1987). [c] Lamer (1993). [d] Baudot and Marin (1996, 1997). [e] Experimental data (Souchon, personal communication). [f] UNIFAC (Reid et al., 1987).

Table 2. Air−Water Partition Coefficients at 25 °C

molecule	volatile concn in liquid (kg/m^3)	air−water partition K_{aw} at 25 °C[a] calcd	exptl
acetaldehyde	1.10E−03	2.9E−03	2.7E−03
dimethyl sulfide	8.46E−04	8.1E−02	2.5E−02
diacetyl	9.61E−04	5.7E−04	3.9E−04
2,5-dimethylpyrazine	8.37E−03	6.3E−05	5.7E−05
menthone	8.93E−05	6.9E−03	7.1E−03

[a] P^0_{water}(25 °C) = 3123 Pa.

step in the process using theoretical equations. Thermodynamic equations and associated data can be found in the literature (Reid et al., 1987; Sandler, 1989; Gemhling et al., 1991). The data have been incorporated (Baudot, 1997) into a Matlab program (The Matworks Inc.), which contains the liquid−vapor equilibrium properties of ∼100 flavor components in water. To validate such models, it is important to have adequate experimental data. Because aroma volatiles cover such a wide range of physicochemical properties, five volatiles were chosen (Table 1), so that a generalized picture of volatile behavior could be obtained. In dilution experiments, changes occur rapidly and the concentration of volatiles in the headspace was monitored in real time using a direct atmospheric pressure ionization mass spectrometer (API-MS) technique (Linforth and Taylor, 1998) with the data point periodicity limited only by the MS sampling rate (typically 0.1 Hz). Previous work in this area has been limited by analytical constraints, that is, the need to sample gas over short periods of time to concentrate the sample sufficiently for GC analysis.

Because the model was developed with unstirred solutions initially, it can also be applied to viscous solutions and gels, for which the effect of volatile mass transfer in the "liquid" and solid phases on release behavior will be more significant.

MATERIALS AND METHODS

Materials. Acetaldehyde, dimethyl sulfide, diacetyl, 2,5-dimethylpyrazine, and menthone were obtained from Aldrich (Gillingham, U.K.). The solutions were prepared in distilled water at low volatile concentrations (from 1×10^{-3} to 1×10^{-4} kg/m^3; see Table 2). The aroma compounds were highly diluted in aqueous solutions, such that there was an insignificant effect of volatiles on the water activity coefficient and the chances of any interaction between the volatiles were minimized.

Static Equilibrium and Headspace Dilution Analysis. Solutions (100 mL) were placed in a glass Schott bottle (123 mL; Fisher, Loughborough, U.K.), without stirring, and sealed with a lid that allowed both removal of headspace samples and introduction of diluting air. Sealed bottles were equilibrated at 25 °C, and then headspace was sampled into the API-MS at 10−70 mL/min using a gas-phase interface (Linforth and Taylor, 1998). Operating conditions were as follows: cone voltages (see Table 1); corona pin voltage at 4 kV; ion dwell time = 0.25 s. The MS was calibrated by introduction of hexane solutions of the volatiles into the air stream, followed by calculation to express concentrations as milligrams per cubic meter.

Modeling. The equations for the various steps in the mechanistic approach (listed under Results) were incorporated into a program written under Matlab (The Matworks Inc.). The change in headspace concentration with time could be predicted for different molecules depending on their physical properties and the operating conditions of the system.

RESULTS AND DISCUSSION

Mechanistic Model Development: Equilibrium Headspace. When the sample is at equilibrium with air in the sealed bottle, the concentration of a volatile i in the gas phase (C_g^i in kg/m^3) is entirely due to partition between the liquid and the gas phases and can be defined as

$$K_{gl}^i = C_i^g / C_i^l \quad (1)$$

where K_{gl}^i is the gas−liquid partition coefficient for the compound i (as, for example, K_{aw} between air and water) and C_i^l is the concentration of the volatile i in the liquid phase (kg/m^3). This equation was used to calculate K_{aw} from experimental data as the volatile concentrations in the liquid and in the gas phase at equilibrium were the parameters measured. The partition coefficient can also be expressed as a function of the thermodynamic properties of the compounds present:

$$K_{gl}^i = \left(\frac{\gamma_i P_i^0(T)}{P_T}\right)\frac{\bar{V}_l}{\bar{V}_g} \quad (2)$$

In eq 2 $P_i^0(T)$ is the vapor pressure for the pure component i (Pa), P_T is the total pressure in the gas phase (Pa), and $\bar{V}_l$ and $\bar{V}_g$ are the molar volumes of the liquid and gas phases, respectively (m^3/mol). If the volatile is highly diluted in the liquid phase, the activity coefficient γ_i can be assumed to be independent of the concentration of the volatile in the liquid and is equal to a constant value γ_l^∞ (the activity coefficient at infinite dilution). In this case, the product $\gamma_l^\infty P_i^0(T)$ is a constant (Henry's constant), so that the value of K_{gl}^i depends only on the temperature.

The five aroma compounds chosen for this study covered a wide range of thermodynamic values (Table 1). For instance, the vapor pressure $P_i^0(T)$ ranged from 4.4×10^1 (for menthone) to 1.2×10^5 (acetaldehyde). The activity coefficient at infinite dilution γ_l^∞ lay in the range 10^1-10^4, with acetaldehyde (a relatively hydrophilic compound) having a value of 3.8, whereas the more hydrophobic molecules (e.g., menthone) have higher values. Henry's constant, which represents the volatility of the compound, also showed a wide range,

with dimethyl sulfide being the most volatile and 2,5-dimethylpyrazine the least volatile compound.

Modeling Dynamic Headspace Dilution. When the equilibrium was disturbed and the headspace diluted with air under isothermal conditions, it was assumed that the partition coefficient remained constant and was independent of the volatile concentration. It was also assumed that, in each phase, there was a small interfacial layer in which the concentration of volatile was different from those in the bulk liquid and gas phases. In the bulk liquid phase, the concentration of volatile was uniform and could be considered constant over the short time course of the experiments. In the bulk gas phase, the concentration changed with time but was considered uniform at any one time throughout the phase. The concentration of the volatile in the gas (air) phase above the sample is the result of a mass balance between release from the liquid phase and removal in the flow of air passing through the cell:

$$V_r[dC_i^g(t)/dt] = J_i(t)A - D_g C_i^g(t) \quad (3)$$

In eq 3 V_r is the volume of the whole gas compartment (m^3), A, the liquid−gas interface area (m^2), and D_g, the gas flow rate through the cell (m^3/s).

Moreover, the expression of the mass flux (J_i) at time t is given by

$$J_i = k[K_{gl}^i C_i^l(t) - C_i^g(t)] \quad (4)$$

and the overall mass transfer coefficient (k in m/s) includes the transport through the liquid phase (k_l) and through the gas phase (k_g). In this model there are three steps that contribute to the overall mass transfer coefficient (k). Initially, there is the mass transfer from the bulk liquid phase to the interface, which is followed by equilibrium at the interface and then by a mass transfer from the interface into the bulk gas phase. The overall process was modeled with the three steps in sequence giving

$$\frac{1}{k} = \frac{1}{k_g} + \frac{K_{gl}^i}{k_l} \quad (5)$$

The expression of the concentration in the gas phase (C_i^g) as a function of time (t) is the result of eqs 3 and 4:

$$\frac{dC_i^g(t)}{dt} = \frac{kA}{V_r} K_{gl}^i C_i^l(t) - \left(\frac{kA + D_g}{V_r}\right) C_i^g(t) \quad (6)$$

At the same time, the variation of the concentration of the volatile in the liquid phase can be expressed as

$$-\frac{dC_i^l}{dt} = \frac{kA}{V_l}[K_{gl}^i C_i^l(t) - C_i^g(t)] \quad (7)$$

where V_l is the volume of the liquid phase (m^3).

For the experiments carried out with the dynamic headspace dilution method, the limiting conditions were as follows:

- At $t = 0$, the concentrations of volatile in the gas and in the liquid phases are both uniform and constant and equilibrium is achieved: $K_{gl}^i C_i^l(t = 0) = C_i^g(t = 0)$, which is the maximum value of C_i^g.
- The dynamic headspace dilution apparatus used in this study was operated over relatively short times (<10 min) and with a relatively large liquid-phase volume. Under these conditions, the variation of the concentration of the volatile in the bulk aqueous phase was negligible, so eq 7 does not have to be taken into account: $dC_i^l/dt \rightarrow 0$ and whatever the value of t, $K_{gl}^i C_i^l(t) \approx C_i^g(t = 0)$.

Then, eq 6 can be solved easily if K_{gl}^i, k, A, V_r, and D_g are assumed to be constant during an isothermal experiment, leading to the analytical solution which can be written as

$$\mathrm{Ln}[MC_i^g(t) - N] = -Mt + \mathrm{Ln}[(D_g/V_r)C_i^g(t = 0)] \quad (8)$$

with $M = kA + D_g/V_r$ and $N = kA/V_r C_i^g(t = 0)$, two constants for each experiment and each volatile.

Validity of Dilution Method for Determining Equilibrium Headspace. The first step in testing the experimental headspace dilution system was to determine the partition coefficients for the five volatile compounds. Initially, a mixture of the five volatiles was equilibrated and the headspace concentrations were measured using API-MS. Values for K_{aw} were obtained using eq 1. Second, a system was taken to equilibrium and then the headspace diluted with air, and changes in headspace concentration were measured with time. The initial headspace concentration (at time zero) was taken as the equilibrium value, and K_{aw} values for the five compounds were calculated using eq 1. The values determined according to the two experimental methods were identical. These values were then compared with values obtained by calculation from thermodynamic data (eq 2) or taken from the literature. Equation 2 requires values for the vapor pressures and activity coefficients of the five volatiles (see Table 1). Vapor pressure data were obtained, either from the literature or by calculation using the Lee−Kesler−Joback method (Reid et al., 1987). Some activity coefficient data were found in the literature; others were obtained using an experimental method of mutual solubility (Voilley et al., 1977) or by calculation (UNIFAC; Reid et al., 1987).

Table 2 shows the experimental and calculated K_{aw} values obtained (at 25 °C), which were generally in good agreement. Even the values for dimethyl sulfide (8.1×10^{-2} and 2.5×10^{-2}) can be considered close, as experimental determination of K_{aw} for this compound is notoriously difficult because of its high volatility. For instance, Van Boekel and Lindsay (1992) determined a K_{aw} of 1.7×10^{-1} for this compound and noted that their value "deviated somewhat" from the value of 6×10^{-2} quoted by Land (1979). The close agreement between theoretical and experimental K_{aw} values also showed that, despite measurement of K_{aw} with all five volatiles present in solution at the same time, the properties of each volatile compound were not significantly modified by the other volatiles at the concentrations used. From these data, it was concluded that the dynamic headspace dilution method could provide a reliable measure of K_{aw}. Moreover, if the system was used to study viscous biopolymer solutions, where the biopolymers might bind the volatiles, the degree of binding could be readily measured by comparison of the K_{aw} values for the volatile in water and the volatile in the biopolymer solution.

Factors Affecting Release in This System. Equation 6 shows the relationship between the factors controlling release in the system. Considering the application modeled, the values for the area of the food

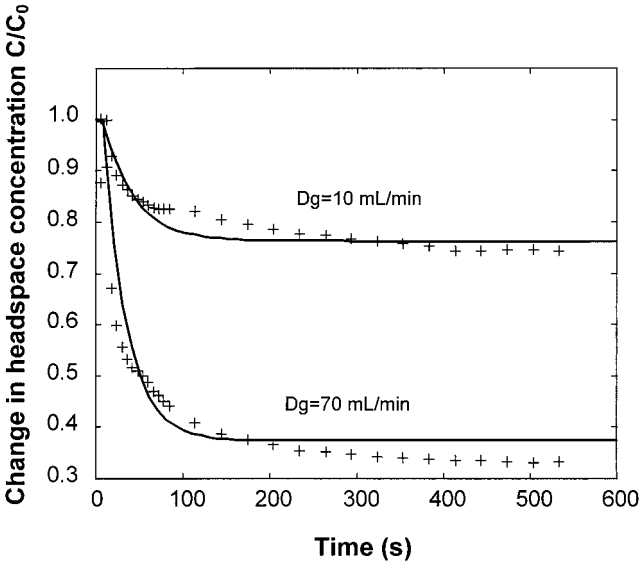

Figure 1. Experimental (+) and calculated (−) release curves for acetaldehyde at different dilution flow rates. Change in headspace concentration is expressed as a fraction of the initial (C_0) value. Operating conditions: $T = 25$ °C; $K_{aw} = 2.7 \times 10^{-3}$; $k_l = 2.5 \times 10^{-6}$ m/s; $A = 1 \times 10^{-3}$ m^2; $V_r = 50 \times 10^{-6}$ m^3.

(A), the volume of the headspace (V_r), the gas−liquid partition coefficient (K_{gl}), and the concentration of volatile in the liquid (C_l) can be taken as constant for one volatile. The change in headspace concentration is then mainly driven by the gas flow (D_g) and the overall mass transfer coefficient (k) during the dynamic headspace dilution method.

Effect of Gas Flow (D_g). To provide further evidence that the model was valid, flow rate was varied and experimental and calculated release curves were compared. For the calculated curves, it was assumed that changing the flow rate between 10 and 70 mL/min had no significant effect on the mass transfer coefficients. Figure 1 shows the calculated and experimental release curves for acetaldehyde under two different dilution flow rates. Changing the flow rate changes the rate at which the headspace concentration decreases, but the experimental and calculated curves for both flow rates show good fit. Figure 1 shows that the concentration in the gas phase decreased more rapidly at high flow rates (70 mL/min) than at low flow rates (10 mL/min). In the system tested in this study, increasing the flow rate has a significant effect on the decrease of the gas concentration as well as the plateau value. It should be stressed that the above conclusions apply to the system described here and care should be taken when they are compared to other systems. For example, Harrison (1998) stated that gas flow rates in his model for volatile release in-mouth had no effect on release. However, his model also included the effect of volatile dilution by a simulated saliva flow, and this was the limiting mechanism for release under the conditions chosen to simulate the mouth.

Mass Transfer Coefficient for the Different Aroma Compounds in the Gas Phase. Because k depends on the mass transfer in the liquid and gas phases, plus a contribution from the air−water partition coefficient (eq 5), the values for these parameters and the effects of flow rate on these parameters (when appropriate) were determined. Dilution of the headspace causes concentration changes in the gas phase and, for convenience, most experimental systems use high gas flows and low volumes of headspace so that the gas phase is well mixed. This reduces variation in the volatile concentration in the gas phase and allows good fitting of the experimental data to the model as noise is minimized. In our system, the operating parameters were set so that the headspace was replaced around one to three times a minute and the experiment was run over periods of 10 min. Typical run-to-run variation was low, with a percentage coefficient of variation (SD × 100/mean) below 8%.

The model took into account the distribution of the volatile throughout the gas phase, which is a function of the mass transfer coefficient (k_g). This parameter can be predicted from the Levêque or the Chilton−Colburn equation, providing the molecular diffusivity of the volatile in air (Wilke and Lee relation), the hydrodynamic operating conditions (Reynolds number), and the shape of the cell are known (Reid et al., 1987). Table 3 shows the calculated and experimentally determined mass transfer coefficients in air (k_g) for the five volatiles. Theoretical values were first calculated using two different Reynolds numbers (25000 and 500), which represent turbulent and laminar flow conditions, respectively. The values for k_g at these extremes of flow conditions show an order of magnitude difference (Re = 25000, $k_g \sim 10^{-2}$ m/s; Re = 500, $k_g \sim 10^{-3}$ m/s). The calculated values of k_g for the five compounds were very similar for both Reynolds numbers [Re = 25000, $(2.5-7.1) \times 10^{-2}$; Re = 500, $(2.3-4.0) \times 10^{-3}$]. The theoretical values for k_g obtained under turbulent conditions were in the same range reported for other small chemical compounds in an air phase (Reid et al., 1987).

Experimental values for k_g were then derived by fitting the experimental curve observed during the dynamic headspace dilution with the theoretical release equations above. Figure 2 contains the experimental and model curves obtained when the concentration has been normalized so that the five compounds can be

Table 3. Calculated and Experimental Mass Transfer Coefficients in the Liquid Phase and in the Gas Phase for Different Reynolds Numbers[a]

	mass transfer coeff (m/s)			
	gas-phase k_g			liquid-phase k_l
molecule	calcd[b] (Re = 25000)	calcd[c] (Re = 500)	exptl[d]	exptl[d]
acetaldehyde	4.0E−02	7.2E−03	3.0E−02	2.5E−06
dimethyl sulfide	3.4E−02	6.2E−03	3.0E−02	2.5E−06
diacetyl	3.2E−02	5.7E−03	3.0E−02	2.0E−06
2,5-dimethylpyrazine	2.7E−02	5.0E−03	3.0E−02	3.0E−06
menthone	2.3E−02	1.2E−03	3.0E−02	1.5E−06

[a] Concentration of volatiles was the same as in Table 2. Operating conditions were as follows: $T = 25$ °C, $A = 1 \times 10^{-3}$ m^2, $V_r = 50 \times 10^{-6}$ m^3, $D_g = 70$ mL/min. [b] Data calculated with the Chilton−Colburn equation (Reid et al., 1987). [c] Data calculated with the Levêque equation (Reid et al., 1987). [d] Values obtained by fitting experimental curve and modeling eq 8.

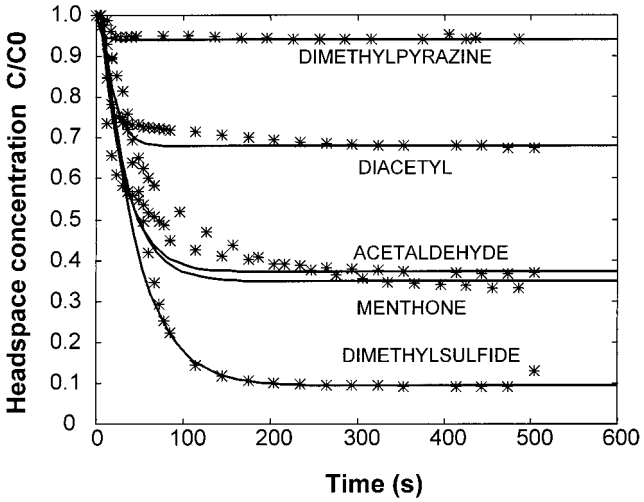

Figure 2. Change in volatile headspace concentration when diluted with air. The experimental data (stars) and the model fitted to the experimental data (solid line) are shown for the five volatile compounds. Change in headspace concentration is expressed as a fraction of the initial concentration C_0. Operating conditions for the system: $T = 25$ °C; $A = 1 \times 10^{-3}$ m^2; $V_r = 50 \times 10^{-6}$ m^3; $D_g = 70$ mL/min.

compared more easily. The curves show a reasonable degree of fit for all five compounds. The experimental values for k_g obtained with a flow rate of 70 mL/min are shown in Table 3 in the k_g experimental column and demonstrate that turbulent conditions exist in the system under these operating parameters. Again, no significant differences in the values of k_g were observed for the five volatiles. Values for k_g were also obtained for flow rates of 10 and 30 mL/min, and these, too, corresponded to high Reynolds number conditions (data not shown). This is not surprising given that the headspace volume in the bottle was 23 mL and the airflows were between 10 and 70 mL/min, leading to a rapid turnover of gas in the headspace per unit time.

As explained above, these operating parameters were chosen to obtain good mixing of the headspace in experimental conditions so that the volatile concentrations would be uniform throughout the gas phase. In systems where food packages are opened and the volatiles are diluted with surrounding air, the flow conditions could be considered as low laminar flow. Overbosch et al. (1991) reported a Reynolds number of 500 for the gas flow in "real mouth conditions", and a similar value seems reasonable for the situation when a food package is opened.

Mass Transfer Coefficient for the Different Volatile Compounds in the Liquid Phase. Experimental values for the apparent mass transfer coefficient (k_l) were derived from fitting the experimental curve during dilution of the headspace (Figure 2) with the theoretical release equations. The values obtained were characteristic of very low Reynolds number because mixing in the liquid phase is substantially lower than in the gas phase. The type of molecule studied had little effect on the experimental value of the apparent mass transfer coefficient in water (Table 3), but the temperature and the properties of the medium (viscosity of the liquid) would play a more important role.

Factors Governing Overall Mass Transfer. From eq 5, the overall mass transfer value depends on mass transfer in the gas and liquid phases with a contribution from K_{aw}. It has been shown that mass transfer in the gas phase depends on the Reynolds number, whereas mass transfer in the liquid phase remains fairly constant in the defined system. Values for the overall mass transfer (k) were calculated using the values of K_{aw}, k_l, and k_g obtained above. Table 4 shows the effect of two different Reynolds numbers on k. When the value of K_{aw} is low ($<10^{-3}$), the second term in eq 5 becomes less significant and the first term (the reciprocal of k_g) is the dominant feature. At values around 10^{-3}, both terms contribute to the overall mass transfer, but above this value, the second term dominates and mass transfer is controlled by the partition coefficient. Translating this into the behavior of individual compounds in this system, 2,5-dimethylpyrazine release is affected by the Reynolds number in the gas phase but dimethyl sulfide

Table 4. Effect of Gas-Phase Hydrodynamic Regime on Overall Mass Transfer Coefficient for the Five Compounds[a]

compound	air−water partition coeff (K_{aw})	overall mass transfer coefficient (k)	
		Re = 500	Re = 25000
dimethylpyrazine	5.70E−05	4.57E−03	1.78E−02
diacetyl	3.90E−04	2.70E−03	4.42E−03
acetaldehyde	2.70E−03	8.20E−04	9.05E−04
menthone	7.10E−03	1.80E−04	2.09E−04
dimethyl sulfide	2.50E−02	9.84E−05	9.97E−05

[a] Reynolds numbers of 500 and 25000 represent laminar and turbulent flow, respectively. The overall mass transfer coefficient was calculated using eq 5 and data from Tables 2 and 3.

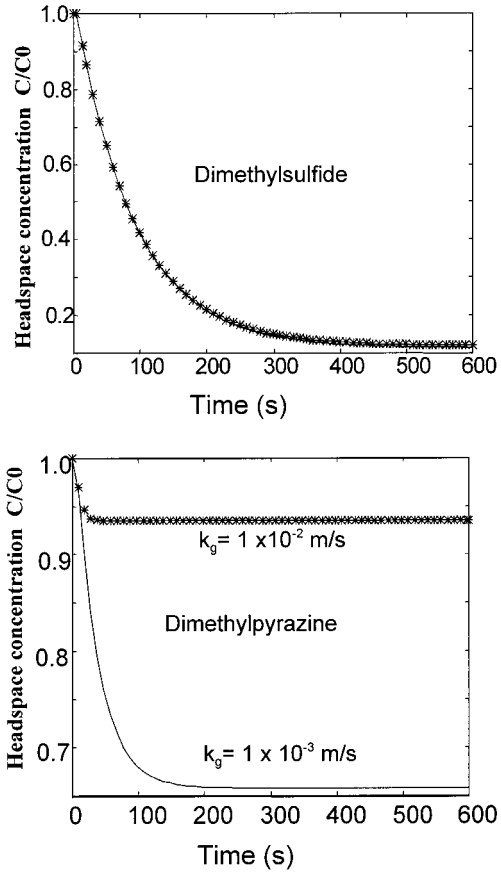

Figure 3. Effect of k_g on release of dimethyl sulfide and dimethylpyrazine at Reynolds numbers representing turbulent (Re = 25000, $k_g = 1 \times 10^{-2}$ m/s) and laminar (Re = 500, $k_g = 1 \times 10^{-3}$ m/s) flow. For both compounds $k_l = 1.5 \times 10^{-6}$ m/s, $A = 1 \times 10^{-3}$ m^3, $D_g = 30$ mL/min, and $V_r = 50 \times 10^{-6}$ m^3. For dimethyl sulfide, $K_{aw} = 2.5 \times 10^{-2}$ and for dimethylpyrazine, $K_{aw} = 5.7 \times 10^{-5}$.

release is governed entirely by K_{aw}, irrespective of Reynolds number in the gas phase. The modeled release curves for the two volatiles under both conditions (assuming constant flow conditions) are shown in Figure 3.

Conclusion. The experimental system delivered high-quality data, which allowed the release process to be modeled. The model release curves fitted the observed data well, and comparison of partition coefficients from the system and from calculation show satisfactory agreement. Using the model, the relative effects of partition coefficient and Reynolds number could be investigated and, for compounds with K_{aw} around 10^{-5}, the gas flow conditions were shown to influence the rate of release significantly. In real volatile release situations, the hydrodynamic regime in the gas phase could have a significant effect on the release of certain volatile components and the volatile profile sensed by consumers. Studies are underway to provide suitable experimental data to confirm the predicted Reynolds number phenomenon under a wide range of hydrodynamic conditions and from viscous and gelled biopolymer solutions.

ACKNOWLEDGMENT

M.M. is grateful to INRA (France) for a sabbatical period spent at the Division of Food Sciences, University of Nottingham, U.K.

LITERATURE CITED

Baudot, A. Pervaporation et condensation étagée, application à l'extraction de composés d'arômes. Thèse de Doctorat, Institut National Agronomique Paris-Grignon, France, 1997.

Baudot, A.; Marin, M., Dairy aroma compounds recovery by pervaporation. *J. Membrane Sci.* **1996**, *120*, 207−220.

Baudot, A.; Marin, M. Pervaporation of aroma compounds: comparison of membrane performances with vapor-liquid equilibria and engineering aspect of process improvement, food and bioproducts processing, *Trans. Inst. Chem. Eng. C* **1997**, *75*, 117−142.

Chaintreau, A.; Grade, A.; Munozbox, R. Determination of partition coefficients and quantitation of headspace volatile compounds. *Anal. Chem.* **1995**, *67*, 3300−3304.

Darling, D. F.; Williams, D.; Yendle, P. Physicochemical interactions involved in aroma transport processes from solutions. In *Interactions of Food Components*; Birch, G. G., Lindley, M. G., Eds.; Elsevier Applied Science: London, U.K., 1986; pp 165−188.

Gemhling, J.; Onken, U.; Artl, W.; Grenheuzer, P.; Weidlich, U.; Koble, B.; Rarey, J. *Vapor-Liquid Equilibrium Data Collection*; Dechema: Dortmund, Germany, 1991; Part 1.

Harrison, M. Effect of breathing and saliva flow on flavor release from liquid food. *J. Agric. Food Chem.* **1998**, *46*, 2727−2735.

Lamer, T. Extraction de composés d'arômes par pervaporation, relation entre les propriétés physico-chimiques des substances d'arômes et leurs transferts à travers des membranes à base de polydiméthylsiloxane. Thèse de Doctorat, Université de Bourgogne, Dijon, France, 1993.

Land, D. G. Some factors influencing the perception of flavor-contributing substances in food. In *Progress in Flavour Research*; Nursten, H. E., Ed.; APS: London, U.K., 1979; pp 53−66.

Linforth, R. S. T.; Taylor, A. J. Apparatus and methods for the analysis of trace constituents in gases. Eur. Patent 97305409.1, Jan 21, 1998; Bulletin 1998/04.

Overbosch, P.; Afterof, W. G. M.; Haring, P. G. M. Flavor release in the mouth. *Food Rev. Int.* **1991**, *7*, 137−184.

Plug, H.; Haring, P. The influence of food-ingredient interactions on flavor perception. *Food Qual Pref.* **1994**, *5*, 95−102.

Reid, R. C.; Prausnitz, J. M.; Poling, B. E. *Properties of Gases and Liquids*; McGraw-Hill: New York, 1987.

Sandler, S. I. *Chemical and Engineering Thermodynamics*, 2nd ed.; Wiley: New York, 1989.

Taylor, A. J. Physical chemistry of flavor. *Int. J. Food Sci. Technol.* **1998**, *33*, 53−62.

Taylor, A. J.; Linforth, R. S. T.; Baek, I.; Brauss, M.; Davidson, J. M.; Gray, D. A. Flavor release and flavor perception. In *Advances in Flavor Chemistry and Technology*; Risch, S. J., Ho, C.-T., Eds.; American Chemical Society: Washington, DC, 1999; in press.

VanBoekel, M. A. J. S.; Lindsay, R. C. Partition of cheese volatiles over vapor, fat and aqueous phases. *Neth. Milk Dairy J.* **1992**, *46*, 197−20.

Voilley, A.; Simatos, D.; Loncin, M. Gas-phase concentration of volatiles in equilibrium with a liquid aqueous phase. *Lebens. Wiss. Technol.* **1977**, *10*, 45.

Received for review May 7, 1999. Revised manuscript received August 16, 1999. Accepted September 2, 1999. I .B. was funded by a U.K. Government MAFF/BBSRC LINK scheme and a Consortium of industrial partners that included Firmenich, Micromass, and Stable Micro Systems.

JF990470G